Abstracta

Ano XVII - N. 02

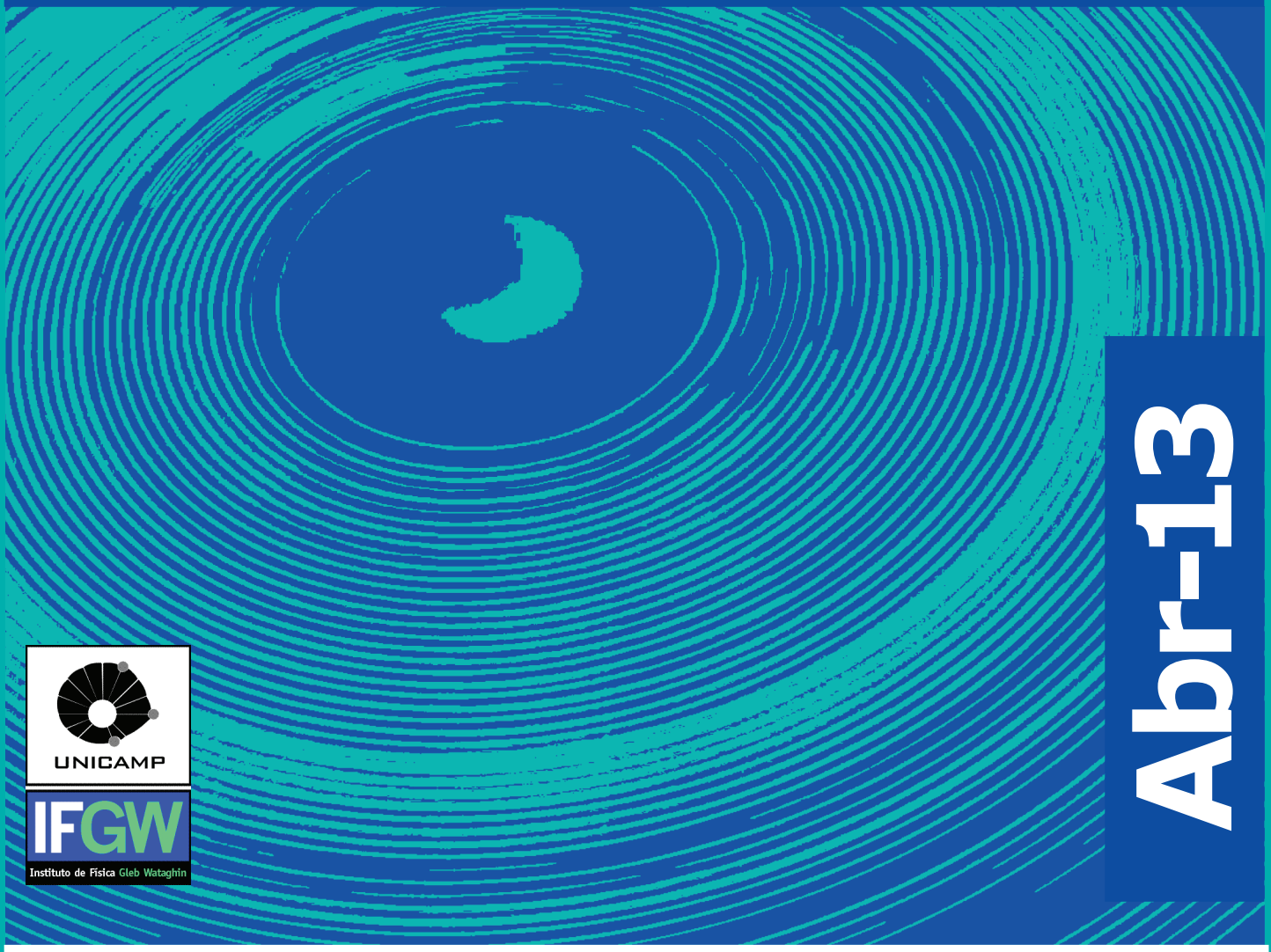

Abr-13

UNICAMP

IFGW
Instituto de Física Gleb Wataghin

Trabalhos Publicados
P067-13 à P106-13

Proceedings
P107-13 à P108-13

Patentes
Pa001-13

Defesas de Dissertações do IFGW - D002-13 à D009-13

Defesas de Teses do IFGW - T003-13 à T004-13

Trabalhos Publicados

[P067-2013] "A novel technique for tailored surface modification of dental implants a step wise approach based on plasma immersion ion implantation"

Meirelles, L.; Uzumaki, E. T.; Lima, J. H. C.; Muller, C. A.; Albrektsson, T.; Wennerberg, A.; **Lambert, C. S.***

Objectives A novel technique based on plasma immersion ion implantation (PIII) is presented to modify titanium implant surfaces. Materials and methods Initially, the implants are cleaned with argon to remove contaminants and the nanostructures are created by the bombardment of the surface with a mix of noble gases. Desired crystal structure of the titanium is obtained by the implantation of oxygen on the contaminant-free surface with particular nanostructures. Results In this study, turned implants modified by PIII revealed a high density of rutile-TiO2 nanostructures. Turned implants used as control revealed mainly microstructures and amorphous crystal structure. Surface roughness values were similar at the microscale for both turned and turned+PIII implants. Bone response was evaluated by removal torque tests of implants placed in the rabbit tibia and femur. After 4weeks of healing, turned+PIII demonstrated higher removal torque values (P=0.001) compared to turned implants. Conclusions The presence of rutile-TiO2 nanostructures may explain the improved bone formation to turned+PIII implants.

Clinical Oral Implants Research 24[4], 461-467, 2013. DOI: 10.1111/j.1600-0501.2011.02352.x

[P068-2013] "Analysis of crosstalk between 10 Gb/s x 64 channels in two-pump fiber optical parametric amplifier"

Callegari, F. A.*; Marconi, J. D.*; Fragnito, H. L.*

We present a numerical study of 64 signals amplified by a two-pump fiber optical parametric amplifier. The amplifier was alternatively simulated with two fibers with different values of nonlinear coefficient but the same length. The gain remained constant in both cases. The performance of the amplifier is improved when it is designed with the fiber of lower nonlinear coefficient. Also, it was observed that the performance of the amplifier is strongly dependent on channel separation.

Microwave And Optical Technology Letters 55[4], 926-929, 2013. DOI: 10.1002/mop.27408

[P069-2013] "Anisotropic flow of charged hadrons, pions and (anti-)protons measured at high transverse momentum in Pb-Pb collisions at root S-NN=2.76 TeV"

Abelev, B.; Adam, J.; Adamova, D.; Adare, A. M.; Aggarwal, M. M.; Rinella, G. A.; Agocs, A. G.; Agostinelli, A.; **Chinellato, D. D.*; Dash, A.*; Takahashi, J.***; et al.
ALICE Collaboration

The elliptic, v(2), triangular, v(3), and quadrangular, v(4), azimuthal anisotropic flow coefficients are measured for unidentified charged particles, pions, and (anti-)protons in Pb-Pb collisions at root S-NN = 2.76 TeV with the ALICE detector at the Large Hadron Collider. Results obtained with the event plane and four-particle cumulant methods are reported for the pseudo-rapidity range vertical bar eta vertical bar < 0.8 at different collision centralities and as a function of transverse momentum, p(T), out to p(T) = 20 GeV/c. The observed non-zero elliptic and triangular flow depends only weakly on transverse momentum for p(T) > 8 GeV/c. The small p(T) dependence of the difference between elliptic flow results obtained from the event plane and four-particle cumulant methods suggests a common origin of flow fluctuations up to p(T) = 8 GeV/c. The magnitude of the (anti-)proton elliptic and triangular flow is larger than that of pions out to at least p(T) = 8 GeV/c indicating that the particle type dependence persists out to high p(T).

Physics Letters B 719[1-3], 18-28, 2013. DOI: 10.1016/j.physletb.2012.12.066

[P070-2013] "Anomalous hysteresis as evidence for a magnetic-field-induced chiral superconducting state in LiFeAs"

Li, G.; **Urbano, R. R.***; Goswami, P.; Tarantini, C.; Lv, B.; Kuhns, P.; Reyes, A. P.; Chu, C. W.; Balicas, L.

Magnetometry measurements in high-quality LiFeAs single crystals reveal a change in the sign of the magnetic hysteresis in the vicinity of the upper critical field H-c2, from a clear diamagnetic response dominated by the pinning of vortices to a considerably smaller net hysteretic response of opposite sign, which disappears at H-c2. If the diamagnetic response at high fields results from pinned vortices and associated screening supercurrents, this sign change must result from currents circulating in the opposite sense, which give rise to a small field-dependent magnetic moment below H-c2. This behavior seems to be extremely sensitive to the sample quality or stoichiometry, as we have observed it only in a few fresh crystals, which also display the de Haas van Alphen effect. We provide arguments against the surface superconductivity, the flux compression, and the random pi junction scenarios, which have been previously put forward to explain a paramagnetic Meissner effect, below the lower critical field H-c1. The observed anomalous hysteresis at high fields will be compatible with the existence of chiral gap wave functions, which possess a field-dependent magnetic moment. Within a Landau-Ginzburg framework, we demonstrate how a (d(x2-y2) + id(xy)) or a (p(x) + ip(y)) chiral superconducting component can be stabilized in the mixed state of s(+/-) superconductor, due to the combined effects of the magnetic field and the presence of competing pairing channels. The realization of a particular chiral pairing depends on the microscopic details of the strengths of the competing pairing channels.

Physical Review B 87[2], 024512, 2013. DOI: 10.1103/PhysRevB.87.024512

[P071-2013] "Atomic surface structure of graphene and its buffer layer on SiC(0001): A chemical-specific photoelectron diffraction approach"

de Lima, L. H.*; de Siervo, A.*; Landers, R.*; Viana, G. A.*; Goncalves, A. M. B.; Lacerda, R. G.; Haeberle, P.

We report a chemically specific x-ray photoelectron diffraction (XPD) investigation using synchrotron radiation of the thermally induced growth of epitaxial graphene on the 6H-SiC(0001). The XPD results show that the buffer layer on the SiC(0001) surface is formed by two domain regions rotated by 60 degrees with respect to each other. The experimental data supported by a comprehensive multiple scattering calculation approach indicates the existence of a long-range ripple due the (6 root 3 x 6 root 3) R30 degrees. reconstruction, in addition to a local range buckling in the (0001) direction of the two sublattices that form the honeycomb structure of the buffer layer. This displacement supports the existence of an sp(2)-to-sp(3) rehybridization in this layer. For the subsequent graphene layer this displacement is absent, which can explain several differences between the electronic structures of graphene and the buffer layer.

Physical Review B 87[8], 081403, 2013. DOI: 10.1103/PhysRevB.87.081403

[P072-2013] "Bulk-plasmon polaritons in metamaterial-metamaterial one-dimensional photonic superlattices"

Reyes-Gomez, E.; Cavalcanti, S. B.; de Carvalho, C. A. A.; **Oliveira, L. E.***

We perform a theoretical study of the bulk-plasmon polaritons in one-dimensional photonic superlattices made up of alternate layers of different metamaterials with dispersive dielectric permittivities and magnetic permeabilities for both normal and oblique incidence. We demonstrate that for oblique incidence a finite projection along the growth direction of the electric or magnetic field of the incident wave associated with the transverse-magnetic or transverse-electric modes, respectively, leads to a coupling in each layer of the heterostructure of the photon modes with the bulk electric or magnetic metamaterial plasmons, respectively. Such photon-plasmon coupling gives rise to electric or magnetic longitudinal bulk-plasmon polariton bands in the photonic band structure of the metamaterial-metamaterial superlattice. We also analyze the conditions for suppression of the longitudinal bulk-plasmon polaritons in the photonic band structure and reflection spectra of such metamaterial-metamaterial heterostructures.

Superlattices And Microstructures 54, 96-106, 2013. DOI: 10.1016/j.spmi.2012.10.009

[P073-2013] "Comparative study on the properties of ZnO nanowires and nanocrystalline thin films"

Broitman E.; Bojorge C.; Elhordoy F.; Kent V. R.; **Gadioli G. Z.***; Marotti R. E.; Canepa H. R.; Dalchiele E. A.

The microstructural, morphological, optical and water-adsorption properties of nanocrystalline ZnO thin films and ZnO nanowires were studied and compared. The ZnO thin films were obtained by a sol-gel process, while the ZnO nanowires were electrochemically grown onto a ZnO sol-gel spin-coated seed layer. Thin films and nanowire samples were deposited onto crystalline quartz substrates covered by an Au electrode, able to be used in a quartz crystal microbalance. X-ray diffraction measurements reveal in both cases a typical diffraction pattern of ZnO wurtzite structure. Scanning electron microscopic images of nanowire samples show the presence of nanowires with hexagonal sections, with diameters ranging from 30 to 90 nm. Optical characterization reveals a bandgap energy of 3.29 eV for the nanowires and 3.35 eV for the thin films. A quartz crystal microbalance placed in a vacuum chamber was used to quantify the amount and kinetics of water adsorption onto the samples. Nanowire samples, which have higher surface areas than the thin films, adsorb significantly more water.

Surface & Coatings Technology 213, 59-64, 2012. DOI: 10.1016/j.surfcoat.2012.10.015

[P074-2013] "Comparisons of annual modulations in MINOS with the event rate modulation in CoGeNT"

Adamson, P.; Anghel, I.; Barr, G.; Bishai, M.; Blake, A.; Bock, G. J.; Bogert, D.; **Coelho, J. A. B.*; Escobar, C. O.***; et al.
MINOS Collaboration

The CoGeNT Collaboration has recently published results from a fifteen month data set which indicate an annual modulation in the event rate similar to what is expected from weakly interacting massive particle interactions. It has been suggested that the CoGeNT modulation may actually be caused by other annually modulating phenomena, specifically the flux of atmospheric muons underground or the radon level in the laboratory. We have compared the phase of the CoGeNT data modulation to that of the concurrent atmospheric muon and radon data collected by the MINOS experiment which occupies an adjacent experimental hall in the Soudan Underground Laboratory. The results presented are obtained by performing a shape-free chi(2) data-to-data comparison and from a simultaneous fit of the MINOS and CoGeNT data to phase-shifted sinusoidal functions. Both tests indicate that the phase of the CoGeNT modulation is inconsistent with the phases of the MINOS muon and radon modulations at the 3.0 sigma level.

Physical Review D 87[3], 032005, 2013. DOI:10.1103/PhysRevD.87.032005

[P075-2013] "Controlled route to the fabrication of carbon and boron nitride nanoscrolls: A molecular dynamics investigation"

Perim, E.*; Paupitz, R.; **Galvao, D. S.***

Carbon nanoscrolls (graphene layers rolled up into papyrus-like tubular structures) are nanostructures with unique and interesting characteristics that could be exploited to build several new nanodevices. However, an efficient and controlled synthesis of these structures was not achieved yet, making its large scale production a challenge to materials scientists. Also, the formation process and detailed mechanisms that occur during its synthesis are not completely known. In this work, using fully atomistic molecular dynamics simulations, we discuss a possible route to nanoscrolls made from graphene layers deposited over silicon oxide substrates containing chambers/pits. The scrolling mechanism is triggered by carbon nanotubes deposited on the layers. The process is completely general and can be used to produce scrolls from other lamellar materials, like boron nitride, for instance.

Journal Of Applied Physics 113[5], 054306, 2013. DOI: 10.1063/1.4790304

[P076-2013] "Determination of the effective distribution coefficient (K) for silicon impurities"

Mei P. R.; Moreira S. P.; **Cortes A. D. S.***; Cardoso E.; **Marques F. C*.**

For the production of photovoltaic cells, the silicon purity can be intermediate between metallurgical grade silicon (MG-Si, 98%-99.9% pure) and electronic grade silicon (>99.9999% pure). This silicon, with intermediate purity and that still meets solar cell requirements, is called upgraded metallurgical grade silicon (UMG-Si). One method of producing UMG-Si is applying a controlled solidification process, like unidirectional solidification (heat exchange method), zone melting (or zone refining), or Czochralski growth to MG-Si. These processes use the impurities solubility difference in solid and liquid silicon known as effective distribution coefficient (K). For these reasons, to study the solidification process, it is necessary to determine K for silicon impurities, which is the objective of this study. MG-Si (99.85% purity or 1500 ppm of impurities) was processed by 1 pass of zone melting at 1 mm/min using an electron beam furnace with water cooled copper crucible. The effective distribution coefficient (K) for impurities with Ko <= 10(-1) was found to follow the relation K = 0.03 Ko(-0.063). For boron, K = 0.8. Impurities with Ko between 10(-3) and 10(-8) presented similar effective distribution coefficients (K = 0.07 +/- 0.02), meaning that the effective distribution coefficient of a specific impurity depends on the total amount of impurities. The measured impurities profiles in silicon were compared with those obtained by Pfann's equations using the effective distribution coefficients and showed comparative results.

Journal of Renewable and Sustainable Energy 4[4], 043118, 2012. DOI: 10.1063/1.4739759

[P077-2013] "Dielectric investigations in unconventionally processed TbMnO3 ceramics"

Gotardo, R. A. M.; Zabotto, F. L.; Garcia, D.; Eiras, J. A.; Dias, G. S.; Cotica, L. F.; Santos, I. A.; **Coelho, A. A.***

TbMnO3 ceramics with enhanced dielectric properties were synthesized by an innovative route combining high-energy ball milling and hot-forging sintering. Dielectric investigations reveal the presence of two distinct relaxation processes: one thermally activated mostly due to dipolar effects and other related to the movement of polar clusters or electric dipoles. Long-range polar order was not achieved, as ferroelectricity in TbMnO3 is strongly dependent on the crystallographic direction. A distribution of relaxation times indicates a cooperative response of the electric dipoles.

Scripta Materialia 68[5], 293-296, 2013. DOI: 10.1016/j.scriptamat.2012.10.045

[P078-2013] "Dynamics of the Formation of Carbon Nanotube Serpentines"

Machado, L. D.*; Legoas, S. B.; Soares, J. S.; Shadmi, N.; Jorio, A.; Joselevich, E.; **Galvao, D. S.***

Recently, Geblinger et al. [Nat. Nanotechnol. 3, 195 (2008)] reported the experimental realization of carbon nanotube S-like shaped nanostructures, the so-called carbon nanotube serpentines. We report here results from multimillion fully atomistic molecular dynamics simulations of their formation. We consider one-mu m-long carbon nanotubes placed on stepped substrates with and without a catalyst nanoparticle on the top free end of the tube. A force is applied to the upper part of the tube during a short period of time and turned off; then the system is set free to evolve in time. Our results show that these conditions are sufficient to form robust serpentines and validates the general features of the "falling spaghetti model" proposed to explain their formation.

Physical Review Letters 110[10], 105502, 2013. DOI: 10.1103/PhysRevLett.110.105502 **(Artigo Destaque de Capa)**

[P079-2013] "Enhancing in the performance of dye-sensitized solar cells by the incorporation of functionalized multi-walled carbon nanotubes into TiO2 films: The role of MWCNT addition"

de Morais, A.; Loiola, L. M. D.; Benedetti, J. E.; Goncalves, A. S.; Avellaneda, C. A. O.; **Clerici, J. H.*; Cotta, M. A.***; Nogueira, A. F.

TiO2-MWCNT composite electrodes were prepared by a direct mixing method. The presence of acid-treated multi-wall carbon nanotubes (MWCNT-COOH) into the titanium dioxide (TiO2) photoanode was investigated by Raman spectroscopy and X-ray diffraction (XRD). The morphological properties of the composite photoanodes were analyzed by field emission scanning electron microscopy (FEG-SEM) and atomic force microscopy (AFM). The performance of quasi-solid state dye-sensitized solar cells (DSSC) using TiO2-MWCNT photoanodes was dependent on the MWCNT loading. Compared with a DSSC based on conventional TiO2 electrodes, the TiO2-MWCNT film containing 0.02 wt.% of carbon nanotubes provided an increase of ca. 30% in device's efficiency, which was attributed to an enhanced short-circuit current density (J(sc)). The improvement on J(sc) was correlated with an enhanced interconnectivity between MWCNT-COOH and TiO2 nanoparticles. The carbonaceous materials introduced an alternative electrical conduction pathway which facilitates rapid electron transport in the photoelectrode, as suggested from Kelvin probe force microscopy (KPFM) measurements. At high MWCNT loading, we observed that the energy conversion efficiency decreased due to energy losses from the optical absorption of carbonaceous materials, and also due to an increase in charge recombination.

Journal Of Photochemistry And Photobiology A-Chemistry 251, 78-84, 2013. DOI: 10.1016/j.jphotochem.2012.09.016

[P080-2013] "Improved zircon fission-track annealing model based on reevaluation of annealing data"

Guedes, S.*; Moreira, P. A. F. P.*; Devanathan, R.; Weber, W. J.; **Hadler, J. C.***

The thermal recovery (annealing) of mineral structure modified by the passage of fission fragments has long been studied by the etching technique. In minerals like apatite and zircon, the annealing kinetics are fairly well constrained from the hour to the million-year timescale and have been described by empirical and semi-empirical equations. On the other hand, laboratory experiments, in which ion beams interact with minerals and synthetic ceramics, have shown that there is a threshold temperature beyond which thermal recovery impedes ion-induced amorphization. In this work, it is assumed that this behavior can be extended to the annealing of fission tracks in minerals. It is proposed that there is a threshold temperature, T (0), beyond which fission tracks are erased within a time t (0), which is independent of the current state of lattice deformation. This implies that iso-annealing curves should converge to a fanning point in the Arrhenius pseudo-space (ln t vs. 1/T). Based on the proposed hypothesis, and laboratory and geological data, annealing equations are reevaluated. The geological timescale estimations of a model arising from this study are discussed through the calculation of partial annealing zone and closure temperature, and comparison with geological sample constraints found in literature. It is shown that the predictions given by this model are closer to field data on closure temperature and partial annealing zone than predictions given by previous models.

Physics And Chemistry Of Minerals 40[2], 93-106, 2013. DOI: 10.1007/s00269-012-0550-8

[P081-2013] "In situ immobilization of nickel(II) phthalocyanine on mesoporous SiO2/C carbon ceramic matrices prepared by the sol-gel method: Use in the simultaneous voltammetric determination of ascorbic acid and dopamine"

Barros, S. B. A.; Rahim, A.; Tanaka, A. A.; Arenas, L. T.; **Landers, R.***; Gushikem, Y.

Three carbon ceramic materials with different porosities were prepared by the sol-gel method, using HNO3, HF, and HNO3/HF as catalysts and the surface areas (S-BET) of the products were determined as 246, 201, and 356 m(2) g(-1), respectively. The materials were characterized using N-2 sorption isotherms, scanning electron microscopy, and conductivity measurements. The matrices were used as supports for the in situ immobilization of Ni(II) phthalocyanine (NiPc) on their surfaces. XPS was used to determine the Ni/Si atomic ratios of the NiPc-modified materials. Pressed disk electrodes were prepared with the NiPc-modified matrices, and tested as sensors for dopamine. The electrode prepared using nitric acid showed excellent catalytic activity for the simultaneous determination of ascorbic acid (AA) and dopamine (DA), with sensitivities of 53.02 and 104.17 mu A mmol dm(-3), respectively. Good repeatability was achieved, with R.S.D. values of 3.67% (AA) and 3.53% (DA), as well as high stability.

Electrochimica Acta 87, 140-147, 2013. DOI: 10.1016/j.electacta.2012.09.012

[P082-2013] "Interpretation of the depths of maximum of extensive air showers measured by the Pierre Auger Observatory"

Abreu, P.; Aglietta, M.; Ahlers, M.; Ahn, E. J.; Albuquerque, I. F. M.; Allekotte, I.; Allen, J.; Allison, P.; Almela, A.; **Alves Batista, R.*; Chinellato, J. A.*; Daniel, B.*; de Mello Junior, W. J. M.*; Dobrigkeit, C.*; Escobar, C. O.*; Fauth, A. C.*; Kemp, E.*; Muller, M. A.*; Pakk Selmi-Dei, D.*; Silva, M. Z.***; et al.
Pierre Auger Collaboration

To interpret the mean depth of cosmic ray air shower maximum and its dispersion, we parametrize those two observables as functions of the first two moments of the ln A distribution. We examine the goodness of this simple method through simulations of test mass distributions. The application of the parameterization to Pierre Auger Observatory data allows one to study the energy dependence of the mean ln A and of its variance under the assumption of selected hadronic interaction models. We discuss possible implications of these dependences in term of interaction models and astrophysical cosmic ray sources.

Journal Of Cosmology And Astroparticle Physics [2], 026, 2013. DOI: 10.1088/1475-7516/2013/02/026

[P083-2013] "Kinematical test of large extra dimension in beta decay experiments"

Basto-Gonzalez, V. S.*; Esmaili, A.*; Peres, O. L. G.*

The forthcoming experiments on neutrino mass measurement using beta decay, open a new window to explore the large extra dimension model. The Kaluza-Klein tower of neutrinos in large extra dimension contributes to the Kurie function of beta decay that can be tested kinematically. In addition to providing an alternative approach using just the kinematical properties, we show that KATRIN can probe the compactification radius of extra dimensions down to 0.2 mu m which is better, at least by a factor of two, than the upper limits from neutrino oscillation experiments.

Physics Letters B 718[3], 1020-1023, 2013. DOI: 10.1016/j.physletb.2012.11.048

[P084-2013] "Long-range angular correlations on the near and away side in p-Pb collisions at root S-NN=5.02 TeV"

Abelev, B.; Adam, J.; Adamova, D.; Adare, A. M.; Aggarwal, M.; **Dash, A. K.*; Takahashi, J.***; et. al.
ALICE Collaboration

Angular correlations between charged trigger and associated particles are measured by the ALICE detector in p-Pb collisions at a nucleon-nucleon centre-of-mass energy of 5.02 TeV for transverse momentum ranges within 0.5 < P-T,P-assoc < P-T,P-trig < 4 GeV/c. The correlations are measured over two units of pseudorapidity and full azimuthal angle in different intervals of event multiplicity, and expressed as associated yield per trigger particle. Two long-range ridge-like structures, one on the near side and one on the away side, are observed when the per-trigger yield obtained in low-multiplicity events is subtracted from the one in high-multiplicity events. The excess on the near-side is qualitatively similar to that recently reported by the CMS Collaboration, while the excess on the away-side is reported for the first time. The two-ridge structure projected onto azimuthal angle is quantified with the second and third Fourier coefficients as well as by near-side and away-side yields and widths. The yields on the near side and on the away side are equal within the uncertainties for all studied event multiplicity and p(T) bins, and the widths show no significant evolution with event multiplicity or p(T). These findings suggest that the near-side ridge is accompanied by an essentially identical away-side ridge.

Physics Letters B 719[1-3], 29-41, 2013. DOI: 10.1016/j.physletb.2013.01.012

[P085-2013] "Magnetostriction of Fe100-xVx alloys for 5.2 <= x <= 40.7"

Bormio-Nunes, C.; Paduani, C.; dos Santos, C. T.; Izario Fo, H. J.; **Coelho, A. A.***; Ghivelder, L.

We investigate the magnetostriction of polycrystalline Fe-100 V-x(x) alloys as a function of vanadium content, with values of x varying from 5.2% to 40.7% (at.%V). The lattice parameter curve behavior as a function of vanadium deviates from a linear behavior at x approximate to 10.2 and x approximate to 30.7. Close to x = 10.2 is possible to observe a small lattice contraction and close to x = 30.7 an expansion. The magnetostriction curve as a function of vanadium content shows two maxima at x = 11.8 and 30.7 and has values of 3/2 lambda(s) of 68.8 ppm and 49.3, respectively. The alloys microstructures investigations do not offer enough elements to connect it with magnetostriction. Therefore first-principles calculations were performed and resulted that the lattice contraction at similar to 0.2% of V is due to the formation of strengthened Fe-V interactions associated to stronger hybridization between minority spin d subbands, while the lattice expansion observed in the range 25.5-30.7% of V is associated to the weakening of the Fe-V interaction. As for the case of simulating V-V pairs for the alloy Fe12V4, representative of x = 25.0, we associated the experimental result of the lattice expansion observed in the range among 25.5-30.7% of V to the weakening of the Fe-V interaction. These calculated electronic properties explain the lattice contraction (at x = 10.2) and expansion (x = 25.5-30.7) and are expected to be the sources of the magnetostrictive behavior of these Fe-V alloys.

Journal Of Alloys And Compounds 553, 233-238, 2013. DOI: 10.1016/j.jallcom.2012.11.034

[P086-2013] "Molecular Dynamics simulations of track formation at different ensembles"

Moreira, P. A. F. P.*; Guedes, S.*; Saenz, C. T.; **Hadler, J. C.***

A series of Molecular Dynamics simulations of thermal spikes has been run in zircon. For two different ensembles: microcanonical one and a combination of microcanonical one acting on the simulation core with Langevin one on the side walls of simulation. Depending on the used ensemble, different track-formation threshold energies were found. When the combined ensemble is carried out, the total energy of the simulations varies with the temperature which can influence how annealing fission-track models should deal with the lattice recovery. A fission-track annealing model is tested with the simulation results.

Radiation Measurements 48, 68-72, 2013. DOI: 10.1016/j.radmeas.2012.10.011

[P087-2013] "Omnidirectional suppression of Anderson localization of light in disordered one-dimensional photonic superlattices"

Reyes-Gomez, E.; Cavalcanti, S. B.; **Oliveira, L. E.***

The omnidirectional suppression of Anderson localization of light in a disordered one-dimensional normal-metamaterial photonic superlattice is thoroughly investigated. Analytical conditions relating to the electric-permittivity and magnetic-permeability responses of each slab of the heterostructure are established for the omnidirectional divergence of the localization length of the normal-metamaterial superlattice. The robustness of such conditions with respect to the degree of disorder of the superlattice is also analyzed.

Journal Of Physics-Condensed Matter 25[7], 075901, 2013. DOI: 10.1088/0953-8984/25/7/075901

[P088-2013] "On the effect of Au2+ ion irradiation in an amorphous Fe-Si thin layer synthesized by ion implantation: a high resolution X-ray diffraction study"

de Menezes, A. S.; **Calligaris, G. A.*; Lang, R.***; dos Santos, A. O.; **Cardoso, L. P.***

High resolution X-ray diffraction and synchrotron radiation multiple diffraction were used to investigate the structural effects induced by 5 MeV Au2+ ion irradiation into amorphous Fe-Si thin layers synthesized by Fe+ ion implantation in a Si(001) substrate.

The concentration-depth profile and damage distribution induced by the Fe and Au ions were estimated by Monte-Carlo calculations (TRIM code) and were used to support the obtained experimental results. Grazing incidence X-ray diffraction and reflectivity measurements show the amorphous feature and interface quality of the as-implanted and Au-irradiated samples. Matrix and a distinct Si-distorted region contributions were detected by high resolution (004) rocking curves, as well as by Si(113) asymmetrical reciprocal space mapping patterns, for just the Au-irradiated samples. They have also shown defect distribution on the Si-distorted region interface plane. The exact multiple diffraction condition of the (1 (1) over bar(1) over bar)(1 (1) over bar3) four-beam case was tailored and showed in a single v: phi mapping, through the (1-13) coherent hybrid reflection, all previously detected effects of the Au-irradiation in the Si lattice. It is the first observation of this kind of hybrid reflection in an ion implanted and irradiated Si substrate. From the incidence (omega) and azimuthal (phi) angular positions measured, the Si-distorted region lattice parameters were determined along the in-plane and out-of-plane directions.

Crystengcomm 15[12], 2251-2259, 2013. DOI: 10.1039/c2ce26478a

[P089-2013] "On the role of extracellular polymeric substances during early stages of Xylella fastidiosa biofilm formation"

Lorite, G. S.*; de Souza, A. A.; Neubauer, D.; Mizaikoff, B.; Kranz, C.; **Cotta, M. A.***

The structural integrity and protection of bacterial biofilms are intrinsically associated with a matrix of extracellular polymeric substances (EPS) produced by the bacteria cells. However, the role of these substances during biofilm adhesion to a surface remains largely unclear. In this study, the influence of EPS on Xylella fastidiosa biofilm formation was investigated. This bacterium is associated with economically important plant diseases; it presents a slow growth rate and thus allows us to pinpoint more precisely the early stages of cell-surface adhesion. Scanning electron microscopy and atomic force microscopy show evidence of EPS production in such early stages and around individual bacteria cells attached to the substrate surface even a few hours after inoculation. In addition, EPS formation was investigated via attenuated total reflectance (ATR) Fourier transform infrared spectroscopy (FTIR). To this end, X. fastidiosa cells were inoculated within an ATR liquid cell assembly. IR-ATR spectra clearly reveal EPS formation already during the early stages of X. fastidiosa biofilm formation, thereby providing supporting evidence for the hypothesis of the relevance of the EPS contribution to the adhesion process.

Colloids And Surfaces B-Biointerfaces 102, 519-525, 2013. DOI: 10.1016/j.colsurfb.2012.08.027

[P090-2013] "Partial hydrogenation of benzene on Ru catalysts: Effects of additives in the reaction medium"

Suppino, R. S.; **Landers, R.***; Cobo, A. J. G.

The partial hydrogenation of benzene is an interesting chemical reaction mostly because of cyclohexene, a compound that can be part of the production chain of many other chemicals. In the present work, it was investigated the effects of additives in the reaction medium on the performance of Ru/Al2O3 and Ru/CeO2 catalysts for the partial hydrogenation of benzene in liquid phase. The Ru catalysts were prepared by incipient impregnation or wet impregnation, both from aqueous solution of the precursor RuCl3 center dot xH(2)O. The catalysts prepared by incipient impregnation were reduced at 573 K under H-2 flow, whereas formaldehyde was used to reduce the catalysts prepared by wet impregnation. The solids were characterized by potentiometric titration, N-2 physisorption, SEM, TEM, EDX, XPS and TPR. The catalytic performance in the liquid phase was evaluated using a slurry Parr reactor at 373 K and under 5 MPa of H-2 pressure. The additives studied were the following: ethylenediamine, ethyl acetate, n-methyl-2-pyrrolidone, monoethyleneglycol and monoethanolamine. The results indicate that the Ru/Al2O3 catalyst, prepared by wet impregnation, leads to the highest values of activity and selectivity. The yield of cyclohexene follows the order: monoethanolamine > monoethyleneglycol > n-methyl-2-pyrrolidone >> ethyl acetate > without additive >> ethylenediamine.

Applied Catalysis A-General 452, 9-16, 2013. DOI: 10.1016/j.apcata.2012.11.034

[P091-2013] "Phase transitions and magnetoelectroelastic instabilities in Pb(Fe1/2Nb1/2)O-3 multiferroic ceramics"

Fraygola, B.; Frizon, N.; Lente, M. H.; **Coelho, A. A.***; Garcia, D.; Eiras, J. A.

Magnetoelectric coupling can be observed in multiferroic materials in the regions where magnetic and ferroelectric ordering coexist and in many cases is mediated via lattice strain. Pb(Fe1/2Nb1/2)O-3 (PFN) is a well-known multiferroic, presenting ferroelectric ordering (below T-C = 380 K) and a Neel temperature (antiferromagnetic ordering) T-N = 143 K. However, recent experimental results suggest that PFN can display ferromagnetic ordering at higher temperatures and a still unclear sequence of phase transitions. In this work, high-density PFN ceramics were prepared by a conventional ceramic method. Dielectric, magnetic and anelastic responses were measured as a function of temperature. The experimental results present complementary evidence of anomalies (additional to those which can be directly associated with the reported transitions at T-C and T-N) which cold be associated with a structural phase transition (T similar to 315 K), an antiferromagnetic ferromagnetic phase transition (110 K) and magnetoelectroelastic instabilities around 250 K.

Acta Materialia 61[5], 1518-1524, 2013. DOI: 10.1016/j.actamat.2012.11.029

[P092-2013] "Pseudorapidity Density of Charged Particles in p plus Pb Collisions at root s(NN)=5.02 TeV"

Abelev, B.; Adam, J.; Adamova, D.; Adare, A. M.; Aggarwal, M. M.; Rinella, G. A.; **Dash, A.*; Takahashi, J.***; et al.
ALICE Collaboration

The charged-particle pseudorapidity density measured over four units of pseudorapidity in nonsingle-diffractive p + Pb collisions at a center-of-mass energy per nucleon pair root s(NN) = 5.02 TeV is presented. The average value at midrapidity is measured to be 16.81 +/- 0.71 (syst), which corresponds to 2.14 +/- 0.17 (syst) per participating nucleon, calculated with the Glauber model. This is 16% lower than in nonsingle-diffractive pp collisions interpolated to the same collision energy and 84% higher than in d + Au collisions at root s(NN) = 0.2 TeV. The measured pseudorapidity density in p + Pb collisions is compared to model predictions and provides new constraints on the description of particle production in high-energy nuclear collisions.

Physical Review Letters 110[3], 032301, 2013. DOI: 10.1103/PhysRevLett.110.032301

[P093-2013] "Reconfigurable silicon thermo-optical ring resonator switch based on Vernier effect control"

Fegadolli W. S.; Vargas G.; Wang X.; **Valini F.*; Barea L. A. M.*;** Oliveira J. E. B.; **Frateschi N.***; Scherer A.; Almeida V. R.; Panepucci R. R.

A proof-of-concept for a new and entirely CMOS compatible thermo-optic reconfigurable switch based on a coupled ring resonator structure is experimentally demonstrated in this paper. Preliminary results show that a single optical device is capable

of combining several functionalities, such as tunable filtering, non-blocking switching and reconfigurability, in a single device with compact footprint (similar to 50 mu m x 30 mu m).

Optics Express 20[13], 14722-14733, 2012.

[P094-2013] "Search for narrow resonances and quantum black holes in inclusive and b-tagged dijet mass spectra from pp collisions at root s=7 TeV"

Chatrchyan, S.; Khachatryan, V.; Sirunyan, A. M.; Tumasyan, A.; Adam, W.; Aguilo, E.; Bergauer, T.; Dragicevic, M.; **Chinellato, J.*; Tonelli Manganote, E. J.***; et al.
CMS Collaboration

A search for narrow resonances and quantum black holes is performed in inclusive and b-tagged dijet mass spectra measured with the CMS detector at the LHC. The data set corresponds to 5 fb(-1) of integrated luminosity collected in pp collisions at root s = 7 TeV. No narrow resonances or quantum black holes are observed. Model-independent upper limits at the 95% confidence level are obtained on the product of the cross section, branching fraction into dijets, and acceptance for three scenarios: decay into quark-quark, quark-gluon, and gluon-gluon pairs. Specific lower limits are set on the mass of string resonances (4.31 TeV), excited quarks (3.32 TeV), axigluons and colorons (3.36 TeV), scalar color-octet resonances (2.07 TeV), E-6 diquarks (3.75 TeV), and on the masses of W' (1.92 TeV) and Z' (1.47 TeV) bosons. The limits on the minimum mass of quantum black holes range from 4 to 5.3 TeV. In addition, b-quark tagging is applied to the two leading jets and upper limits are set on the production of narrow dijet resonances in a model-independent fashion as a function of the branching fraction to b-jet pairs.

Journal Of High Energy Physics [1], 013, 2013. DOI: 10.1007/JHEP01(2013)013

[P095-2013] "Selectively coupling core pairs in multicore photonic crystal fibers: optical couplers, filters and polarization splitters for space-division-multiplexed transmission systems"

Gerosa R. M.; **Biazoli C. R.*; Cordeiro C. M. B.***; de Matos C. J. S.

Selective coupling a single pair of cores in a photonic crystal fiber with multiple, initially decoupled, cores is demonstrated through the use of a technique to locally post-process the fiber cross section. Coupling occurs when the hole between the selected core pair is collapsed over a short fiber section, which is accomplished by heating the section while the hole is submitted to an air pressure that is lower than that applied to all other holes in the microstructure. The demonstrated couplers present an estimated insertion loss of similar to 1 dB and exhibit spectral modulations with a depth of up to 18 dB and a high polarization sensitivity that can be exploited for polarization splitting or filtering in space-division-multiplexed optical interconnection and telecommunication links.

Optics Express 20[27], 28981-28988, 2012.

[P096-2013] "Simultaneous measurement of refractive index and temperature using multimode interference inside a high birefringence fiber loop mirror"

Gouveia, C.; **Chesini, G.*; Cordeiro, C. M. B.***; Baptista, J. M.; Jorge, P. A. S.

A fiber optic sensor for simultaneous measurement of refractive index and temperature is presented. The sensing probe is realized by introducing a multimode interference device inside a high birefringence fiber loop mirror resulting in a configuration capable of refractive index and temperature discrimination. The multimode interference peak is sensitive to the surrounding refractive index (90 nm/RIU) and slightly responsive to the temperature (0.01 nm/ degrees C). On the other hand, the birefringent fiber loop mirror is highly sensitive to temperature (2.36 nm/ degrees C) and it has almost no response to refractive index. Using a power ratiometric peak detection scheme, a temperature independent refractive index measurement can be achieved with a resolution of +/- 2.25 x 10(-5) RIU.

Sensors And Actuators B-Chemical 177, 717-723, 2013. DOI: 10.1016/j.snb.2012.11.095

[P097-2013] "Single spin asymmetry AN in polarized proton--proton elastic scattering at root s=200 GeV"

Adamczyk, L.; Agakishiev, G.; Aggarwal, M. M.; Ahammed, Z.; Alakhverdyants, A. V.; Alekseev, I.; **Derradi de Souza, R.*; Takahashi, J.*; Vasconcelos, G. M. S.***; et al.
STAR Collaboration

We report a high precision measurement of the transverse single spin asymmetry A(N) at the center of mass energy root s = 200 GeV in elastic proton-proton scattering by the STAR experiment at RHIC. The A(N) was measured in the four-momentum transfer squared t range 0.003 <= vertical bar t vertical bar <= 0.035 (GeV/c) (2), the region of a significant interference between the electromagnetic and hadronic scattering amplitudes. The measured values of A(N) and its t-dependence are consistent with a vanishing hadronic spin-flip amplitude, thus providing strong constraints on the ratio of the single spin-flip to the non-flip amplitudes. Since the hadronic amplitude is dominated by the Pomeron amplitude at this root s, we conclude that this measurement addresses the question about the presence of a hadronic spin flip due to the Pomeron exchange in polarized proton-proton elastic scattering.

Physics Letters B 719, [1-3], 62-69, 2013. DOI: 10.1016/j.physletb.2013.01.014

[P098-2013] "Stability and Relaxation Mechanisms of Citric Acid Coated Magnetite Nanoparticles for Magnetic Hyperthermia"

de Sousa, M. E.; van Raap, M. B. F.; Rivas, P. C.; Zelis, P. M.; Girardin, P.; Pasquevich, G. A.; Alessandrini, J. L.; **Muraca, D.***; Sanchez, F. H.

Magnetite (Fe3O4) nanoparticles are proper materials for Magnetic Fluid Hyperthermia applications whenever these conjugate stability at physiological (neutral pH) medium and high specific dissipation power. Here, magnetite nanoparticles 9-12 nm in size, electrostatically stabilized by citric acid coating, with hydrodynamic sizes in the range 17-30 nm, and well dispersed in aqueous solution were prepared using a chemical route. The influence of media acidity during the adsorption of citric acid (CA) on the suspension's long-term stability was systematically investigated. The highest content of nanoparticles in a stable suspension at neutral pH is obtained for coating performed at pH = 4.58, corresponding to the larger amount of CA molecules adsorbed by one carboxylate link. Specific absorption rates (SARs) of various magnetite colloids, determined calorimetrically at a radio frequency field of 265 kHz and field amplitude of 40.1 kA/m, are analyzed in terms of structural and magnetic colloid properties. Larger dipolar interactions lead to larger Neel relaxation times, in some cases larger than Brown relaxation times, which in the present case enhanced magnetic radio frequency heating. The improvement of suspension stability results in a decrease of SAR values, and this decrease is even large in comparison with uncoated magnetite nanoparticles. This fact is related to interactions between particles.

Journl of Physical Chemistry C 117[10], 5436-5445, 2013. DOI: 10.1021/jp311556b

[P099-2013] "Strain-Temperature Discrimination Using Multimode Interference in Tapered Fiber"

Andre, R. M.; **Biazoli, C. R.***; Silva, S. O.; Marques, M. B.; **Cordeiro, C. M. B.***; Frazao, O.

Tapering single-mode-multimode-single-mode structures to enhance sensitivity is proposed and experimentally demonstrated. 50-mm-long coreless multimode fiber sections are spliced between single-mode fibers (SMFs) and tapered. They are characterized in strain, and an increase in strain sensitivity is obtained with taper diameter reduction. Sensitivities as high as -23.69 pm/mu epsilon for the 15-mu m taper are attained. Temperature sensitivities also depend on taper diameter. A combination of two different diameter tapered SMF MMF-SMF structures, with cross-sensitivity to strain and temperature, is proposed as a sensing system for the simultaneous measurement of strain and temperature with resolutions of +/-5.6 mu epsilon and +/-1.6 degrees C, respectively. A good condition number of 3.16 is achieved with this sensing structure.

IEEE Photonics Technology Letters 25[2], 155-158, 2013. DOI: 10.1109/LPT.2012.2230617

[P100-2013] "Structural and magnetic behavior of ferrogels obtained by freezing thawing of polyvinyl alcohol/poly(acrylic acid) (PAA)-coated iron oxide nanoparticles"

Moscoso-Londono, O.; Gonzalez, J. S.; **Muraca, D.***; Hoppe, C. E.; Alvarez, V. A.; Lopez-Quintela, A.; Socolovsky, L. M.; **Pirota, K. R.***

Superparamagnetic ferrogels with high swelling ability and potential applications as solvent absorbers and stimuli-responsive drug delivery devices were obtained by a non-toxic and environmentally friendly route based on dispersion of poly(acrylic acid)-coated iron oxide nanoparticles (PAA-coated NPs) in poly(vinyl alcohol) (PVA) solutions followed by freezing-thawing. Presence of carboxylate groups arising from the PAA coating allowed hydrogen bonding formation between NPs and PVA and enabled the synthesis of optically homogenous, superparamagnetic materials formed by a homogenous distribution of NPs diffuse clusters in the PVA matrix. The addition of PAA-coated NPs produced a remarkable increase in crystallinity degree, thermal degradation and swelling percentage respect to the neat matrix, which demonstrates that ferrogels with improved properties can be obtained by this procedure. Thereafter, combination of a cryogenic technique with the use of non-toxic components and magnetic NPs coated by a pH sensitive polymer makes these ferrogels very promising for applications in the biomedical field.

European Polymer Journal 49[2], 279-289, 2013. DOI: 10.1016/j.eurpolymj.2012.11.007

[P101-2013] "Structural, surface, and thermomechanical properties of intrinsic and argon implanted tetrahedral amorphous carbon"

Motta, E. F.*; Viana, G. A.*; Silva, D. S.*; Cortes, A. D. S.*; Freire, F. L.; **Marques, F. C.***

The structural, surface, and thermomechanical properties of intrinsic and argon incorporated tetrahedral amorphous carbon films deposited using the filtered cathodic vacuum arc process are reported. Argon atoms were simultaneously incorporated during the deposition of the films using an argon ion gun in the energy range of 0-180 eV. Contact angle measurements revealed that all of the deposited films are hydrophobic, regardless of the substrate bias voltage that was applied during the depositions. Thermal desorption spectroscopy measurements revealed that high argon bombarding energy favors films that are structurally more compact and thermally more stable. An investigation unbinding the mechanism of argon effusion and intrinsic stress relief is presented.

Journal Of Vacuum Science & Technology A 31[2], 021502, 2013. DOI: 10.1116/1.4774326

[P102-2013] "Study of the Mass and Spin-Parity of the Higgs Boson Candidate via Its Decays to Z Boson Pairs"

Chatrchyan, S.; Khachatryan, V.; Sirunyan, A. M.; Tumasyan, A.; Adam, W.; Aguilo, E.; Bergauer, T.; **Chinellato, J.*; Tonelli Manganote, E. J.***; et al.
CMS Collaboration

A study is presented of the mass and spin-parity of the new boson recently observed at the LHC at a mass near 125 GeV. An integrated luminosity of 17: 3 fb(-1), collected by the CMS experiment in proton-proton collisions at center-of-mass energies of 7 and 8 TeV, is used. The measured mass in the ZZ channel, where both Z bosons decay to e or mu pairs, is 126: 2 +/- 0.6(stat) +/- 0. 2(syst) GeV. The angular distributions of the lepton pairs in this channel are sensitive to the spin-parity of the boson. Under the assumption of spin 0, the present data are consistent with the pure scalar hypothesis, while disfavoring the pure pseudoscalar hypothesis.

Physical Review Letters 110[8], 081803, 2013. DOI: 10.1103/PhysRevLett.110.081803

[P103-2013] "Tests of CMS hadron forward calorimeter upgrade readout box prototype"

Chatrchyan, S.; Khachatryan, V.; Sirunyan, A. M.; Tumasyan, A.; Mossolov, V.; Shumeiko, N.; Cornelis, T.; Junior, W. L. A.; Carvalho, W.; **Chinellato, J.***; Martins, C. O.; Figueiredo, D. M.; **Manganote, E.***; Molina, J.; Mundim, L.; Nogima, H.; Da Silva, W. L. P.; Santoro, A.; Zachi, A.; et al.
CMS HCAL Collaboration

A readout box prototype for the CMS Hadron Forward calorimeter upgrade was built and tested in the CERN H2 beamline. The prototype was designed to enable simultaneous tests of different readout options for the four anode upgrade PMTs, new front-end electronics design and new cabling. The response of the PMTs with different readout options was uniform and the background response was minimal. Multi-channel readout options further enhanced the background elimination. Passing all the electronic, mechanical and physics tests, the readout box proved to be capable of providing the forward hadron calorimeter operational requirements in the upgrade era.

Journal of Instrumentation 7, P10015, 2012. DOI: 10.1088/1748-0221/7/10/P10015

[P104-2013] "The radial pair distribution function for two-dimensional Lennard-Jones systems"

Madeira L.*; Vitiello S. A.*

Properties of two-dimensional Lennard-Jones systems are studied with the aim of introducing the molecular dynamics method. In particular, we give attention to the calculation of the radial distribution function. The good agreement of our results with theory and results of another simulation shows that this is a method not only easy to implement, but also reliable. In addition, we have shown that the molecular dynamics method can help us with the interpretation of results and increase our understanding of them.

Revista Brasileira de Ensino de Física 34[4], 4303, 2012.

[P105-2013] "Transverse Momentum Distribution and Nuclear Modification Factor of Charged Particles in p plus Pb Collisions at root(NN)-N-s=5.02 TeV"

Abelev, B.; Adam, J.; Adamova, D.; Adare, A. M.; Aggarwal, M. M.; Rinella, G. A.; Agnello, M.; Agocs, A. G.; Agostinelli, A.; **Dash, A.*; Takahashi, J.***; et al.

The transverse momentum (pT) distribution of primary charged particles is measured in minimum bias (non-single-diffractive) p + Pb collisions at root(NN)-N-s = 5.02 TeV with the ALICE detector at the LHC. The pT spectra measured near central rapidity in the range 0.5< p(T) < 20 GeV/c exhibit a weak pseudorapidity dependence. The nuclear modification factor R-pPb is consistent with unity for p(T) above 2 GeV/c. This measurement indicates that the strong suppression of hadron production at high p(T) observed in Pb + Pb collisions at the LHC is not due to an initial-state effect. The measurement is compared to theoretical calculations.

Physical Review Letters 110[8], 082302, 2013. DOI: 10.1103/PhysRevLett.110.082302

[P106-2013] "Why entanglement of formation is not generally monogamous"

Fanchini, F. F.; **de Oliveira, M. C.***; Castelano, L. K.; Cornelio, M. F.

Unlike correlation of classical systems, entanglement of quantum systems cannot be distributed at will: if one system A is maximally entangled with another system B, it cannot be entangled at all with a third system C. This concept, known as the monogamy of entanglement, is manifest when the entanglement of A with a pair BC can be divided as contributions of the entanglement between A and B and A and C, plus a term tau(ABC) involving genuine tripartite entanglement and so expected to be always positive. A very important measure in quantum information theory, the entanglement of formation (EOF), fails to satisfy this last requirement. Here we present the reasons for that and show a set of conditions that an arbitrary pure tripartite state must satisfy for the EOF to become a monogamous measure, i.e., for tau(ABC) >= 0. The relation derived is connected to the discrepancy between quantum and classical correlations, tau(ABC) being negative whenever the quantum correlation prevails over the classical one. This result is employed to elucidate features of the distribution of entanglement during a dynamical evolution. It also helps to relate all monogamous instances of the EOF to the squashed entanglement, an entanglement measure that is always monogamous.

Physical Review A 87[3], 032317, 2013. DOI: 10.1103/PhysRevA.87.032317

Proceedings

[P107-13] "Measurements of plasma edge electron temperature and density using visible spectroscopy in NOVA-UNICAMP tokamak"

do Nascimento, F.*; Machida, M.*; Bilbao L.(editor); Minotti F.(editor); Kelly H.(editor)

The electron temperature (T-e) and density (n(e)) at the edge of NOVA-UNICAMP tokamak plasma were determined along the discharge using the concept of particle confinement time (tau(P)) uniqueness and spectroscopic measurements of hydrogen Balmer series emissions. We have used three absolutely intensity calibrated spectrometers with photomultipliers for simultaneous measurements of hydrogen alpha, beta and gamma emissions throughout the discharges. With the use of data from Johnson and Hinnov's table, we have performed an interactive method to find electron temperatures and densities that satisfy the tau(P) uniqueness to obtain the temporal evolution of T-e and n(e) parameters. The results achieved are in agreement with the expected values for these parameters at the edge of the NOVA-UNICAMP tokamak plasma.

Latin American Workshop on Plasma Physics (LAWPP) XIV. Journal of Physics Conference Series. v. 370, 012053, 2012 - Conference on Latin American Workshop on Plasma Physics XIV, NOV 20-25, 2011, Mar del Plata, Argentina.

[P108-2013] "Irreversibility lines and anomalous Meissner effect in Ba(Fe1-xCox)(2)As-2 superconducting crystals"

de Lima O. F.*; de Almeida R. L.*; Garitezi T. M.*; Adriano C.*; Rosa P. F. S.*; Pagliuso P. G.*; Kes P. H.(editor); Rogalla H.(editor).

Magnetization curves were measured in Ba(Fe1-xCox)(2)As-2 crystals grown by an indium flux method. A very different vortex dynamics behavior was found when comparing results for crystals in the underdoped and slightly above the optimal doped regions. The irreversibility line is closer to the upper critical field line in the latter case, which indicates a much strong pinning of vortices for the near optimally doped crystal. Also, field cooled magnetization curves revealed an anomalous Meissner effect, where a diamagnetic response increases with the applied field, in both crystals. Possible mechanisms involving vortex pinning at interfaces or by local magnetic ions are presented.

Superconductivity Centennial Conference (SCC). Superconductivity Centennial Conference. v. 36, 1661-1666, 2011 - SEP 18-23, 2011, Hague, NETHERLANDS. DOI: 10.1016/j.phpro.2012.10.001

Patentes

[Pa-001-2013] "Composição para fabricação de dormentes de concreto reforçado com fibras"

Barbosa, L. C.*; Maia, M. P. F.; Barbosa, M. T. G.; Ludwig, Z. M. C.

Número da Patente ou Registro:(Agência INOVA) BR 10 2013 001653 5
Tipo da Patente: Patente de Invenção
Mês/Ano de Conclusão: 01/2013
INPI/BRASIL

Fonte: SIPEX – Sistema de Informação de Pesquisa e Extensão da Unicamp.
Disponível em: http://www.unicamp.br/sipex/

*** Autores do Instituto de Física "Gleb Wataghin" - IFGW**

Defesas de Dissertações - Mestrado

[D002-13] "Estudo de Correlações Angulares entre Raios Cósmicos de Energias Ultra-Altas Detectados pelo Observatório Pierre Auger".
Aluno: Camile Mendes Castilho
Orientador: Carola Dobrigkeit Chinellato
Data: 22/02/2013.

[D003-13] "Dispositivos em Fibras Ópticas Baseadas em Interferência Multimodal".
Aluno: Edwin German Pinilla Pachon
Orientador: Cristiano Monteiro de Barros Cordeiro
Data: 05/03/2013.

[D004-13] "Utilização da fMRS para o Estudo da Variação de N-acetil-aspartato e N-Acetil-Aspartil-Glutamato Durante a Ativação Cerebral".
Aluno: Ricardo Cesar Giorgetti Landim
Orientador: Gabriela Castellano
Data: 15/03/2013.

[D005-13] "Enviroment-Induced Anisotropy and the Sensitivity of the Radical Pair Mechanism in the Avian Compass".
Aluno: Alejandro Carrillo Lozada
Orientador: Marcos Cesar de Oliveira
Data: 04/04/2013

[D006-13] "Discos Relativísticos Auto-gravitantes: Aspectos de estabilidade e Integrabilidade".
Aluno: Vanessa Pacheco de Freitas
Orientador: Alberto Vazquez Saa
Data: 05/04/2013.

[D007-13] "O Modo Fundamental de Emissão de Ondas Gravitacionais".
Aluno: Gibran Henrique de Souza
Orientador: Anderson Campos Fauth
Data: 30/04/2013.

[D008-13] "Propriedades Magnéticas e Ópticas de Nanopartículas".
Aluno: Guilherme Gorgen Lesseux
Orientador: Carlos Rettori
Data: 06/05/2013.

[D009-13] "Decoerência de Pacote Gaussiano em um Potencial Harmônico".
Aluno: André Cidrim Santos
Orientador: Amir Ordacgi Caldeira
Data: 08/05/2013.

Defesas de Teses - Doutorado

[T003-13] "Estudo da Absorção de Moléculas em Nanofios de Ouro e Nanofios Magnéticos".
Aluno: Ana Paula Favaro Nascimento
Orientador: Edison Zacarias da Silva
Data: 15/03/2013.

[T004-13] "Plataforma fotônica integrada e suas aplicações em estudos de quantum dots e processos biológicos".
Aluno: André Alexandre de Thomaz
Orientador: Carlos Lenz César
Data: 27/03/2013.

Fonte: Portal IFGW/Pós-graduação.
Disponível em: http://portal.ifi.unicamp.br/eventos/eventos-defesas-tese

*** Acesse o portal Abstracta <http://abstracta.ifi.unicamp.br> e faça seu cadastro como Leitor** para receber por email as novidades de cada novo número publicado.

Abstracta

Instituto de Física
Diretor: Prof. Dr. Daniel Pereira
Diretor Associado: Prof. Dr. Newton Cesario Frateschi
Universidade Estadual de Campinas - UNICAMP
Cidade Universitária Zeferino Vaz
13083-859 - Campinas - SP - Brasil
e-mail: secdir@ifi.unicamp.br
Fone: 0XX 19 3521-5300

Publicação

Biblioteca do Instituto de Física Gleb Wataghin
http://portal.ifi.unicamp.br/biblioteca

Diretora Técnica: Sandra Maria Carlos Cartaxo
Coordenador da Comissão de Biblioteca: Prof. Dr. André Koch Torres de Assis

Elaboração
Maria Graciele Trevisan (Bibliotecária)
graciele@ifi.unicamp.br

Projeto Gráfico
ÍgneaDesign

Impressão: Gráfica Central - Unicamp